OPTIC DISK LOCALIZATION USING L_1 MINIMIZATION

Neelam Sinha

IIIT,
Bangalore, India.

R. Venkatesh Babu

SERC, Indian Institute of Science,
Bangalore, India

ABSTRACT

Automatic eye screening for conditions like diabetic retinopathy critically hinges on detection and localization of Optic disk (OD). In this paper, we present a novel scale-embedded dictionary-based method that poses the problem of OD localization as that of classification, carried out in sparse representation framework. A dictionary is created with manually marked fixed-sized sub-images that contain OD at the center, for multiple scales. For a given test image, all sub-images are sparsely represented as a linear combination of OD dictionary elements. A confidence measure indicating the likelihood of the presence of OD is obtained from these coefficients. Red channel and gray intensity images are processed independently, and their respective confidence measures are fused to form a confidence map. A blob detector is run on the confidence map, whose peak response is considered to be at the location of the OD. The proposed method is evaluated on publicly available databases such as DIARETDB0, DIARETDB1 and DRIVE. The OD was correctly localized in 253 out of 259 images, with an average computation time of 3.8 seconds/image and accuracy of 97.6%. Comparisons with two existing techniques are also discussed.

***Index Terms*—** fundal image processing, optic disk detection, sparse representation, l_1-norm minimization

1. INTRODUCTION

The optic disc (OD) is considered to be a very important feature in a retinal fundus image. Automatic OD localization is a critical step in eye image processing, since it serves as a landmark for subsequent diagnostics. Although various disparities in ODs are seen across the population, they are typically characterized by their nearly circular shape and as the convergence region of a network of blood vessels and nerves. OD localization is generally followed by extraction of exudates and lesions, and hence serves as an important initial step for automatic screening for several pathological conditions, such as diabetic retinopathy (DR). Localizing OD also helps in determining other landmarks such as the fovea and macula, which are used in several studies.

2. OD LOCALIZATION METHODS

OD localization methods can broadly be classified as those that utilize the brightness and relatively large size of the OD, while many others have exploited the circular shape of the OD by utilizing the circular Hough Transform. In [1], the authors approximate the OD center as that of the largest brightest connected component in the fundus image. They obtain a binary image including all the bright regions by thresholding the intensity image. Another work that exploits the brightness of the OD pixels was reported in [2]. Here, the authors identify the candidate regions by clustering the brightest pixels in the intensity images. PCA is applied to these candidate regions. In [3] the OD is localized using morphological operations followed by the Hough transform. The method reported in [4] comprises several pre-processing steps, such as binarization for mask generation followed by equalization. Blood vessel segmentation is carried out using matched filter frame-work in order to match the direction of the vessels at the OD vicinity. Some works devise methods by customizing concepts of multi-scale approaches and filtering, for OD detection. The work reported in [5] proposes a method to automatically detect the OD in fundus images in two steps. The OD vessel candidate detection is followed by OD vessel candidate matching. In the first step multi-scale Gaussian filtering, scale production, and double thresholding are carried out to initially extract the directional map of the vessels. The resulting map is thinned and thresholded to eliminate pixels with low intensities, yielding the OD vessel candidates. This is followed by a Vessels Directional Matched Filter (VDMF) of various dimensions. VDMF is applied to the candidates to be matched, and the pixel with the smallest difference is designated the OD center. In [6], the authors report an image processing algorithm for OD localization in low-resolution color fundus images. The authors propose a combination of a Hausdorff-based template matching technique on edge maps, directed by a pyramidal decomposition for large scale object tracking. In the work reported in [7]a deformable model is used for image segmentation that integrates features of region-based and edge-based segmentation techniques. The model is designed such that it is able to fit the edges of the objects and model their inner topology.

For a method to be robust, it has to steer clear of the sensitive pre-processing requirements and assumptions. In the present work, we propose an approach that imposes no restriction of shape, color or contrast. Instead it allows the system to learn the characteristic features of ODs by utilizing a scale-embedded dictionary of sub-images, each of which contains OD at the center. Each test sub-image is expressed as a sparse linear combination of dictionary patterns. Confidence measure obtained from these sparse coefficients indicate the likelihood of the presence of OD.

3. PROPOSED METHOD

The proposed method poses the problem of OD localization as a classification problem where the two competing classes are sub-images of a fixed size such that (i) they contain OD at the center and (ii) they do not contain OD at the center. For a given test image, the objective is to determine which of its constituent sub-images contains OD at its center, thus accomplishing OD localization. The training patterns constitute the dictionary D, with respect to which, each of the testing sub-images is expressed as a sparse linear combination of the dictionary patterns.

3.1. Sparse representation

Given an over-complete dictionary $\mathcal{T}$ in $R^{p\times q}$ where p is the size of feature vector and q is the number of training patterns in the dictionary, the input test sample $\mathbf{y} \in R^{p\times 1}$ is represented as a sparse linear combination of dictionary atoms

$$\mathbf{y} = \mathcal{T}\alpha \tag{1}$$

To obtain the sparsest representation, we need to solve the following optimization problem,

$$\min_{\alpha\in R^p} \|\alpha\|_0 \text{ subject to } \mathbf{y} = \mathcal{T}\alpha$$

where $\| \, . \, \|_0$ denotes the l_0-norm, which counts the number of non-zero entries in a vector. However, this problem is NP-hard, and there is no known procedure for finding the sparsest solution that is significantly more efficient than exhaustively searching through all possible solutions. Recent developments in sparse representation and compressed sensing [8] have led to results that if the optimal solution α is sufficiently sparse then the l_0-norm minimization problem is equivalent to solving the l_1-norm minimization problem :

$$\min_{\alpha\in R^p} \|\alpha\|_1 \text{ subject to } ||\mathcal{T}\alpha - y||_2 \leq \epsilon \tag{2}$$

for an appropriately small value of ϵ. As is well known, this convex optimization problem can be efficiently solved via cone programming [9]. The solution would contain coefficients that are sparse and their magnitudes decay rapidly.

3.2. Dictionary creation

Hand-marked sub-images with OD at the center, at multiple scales, are utilized to create the scale-embedded dictionary. The sub-images are resized to $n_1 \times n_2$ for computational ease. The dictionary elements are obtained by representing these sub-images as a column vector. It is observed that typically the Red channel image suppresses contrast information within the OD, leaving a disk-shaped blob, which is a very important cue for OD detection. On the other hand, the gray intensity images contain contrast within the OD, outlining the cris-cross of blood vessels and nerves. Hence for every chosen sub-image, its red channel image as well as the gray intensity image are used as training patterns in the dictionary. In the choice of sub-images, it is ensured that multiple scales of the OD are represented in order to capture the scale variation of OD across images. Similar-sized matrices with a single non-zero entry for each of the $n_1 \times n_2$ locations are also included in the dictionary to handle noise and artifacts. The process of dictionary creation is summarized in Fig. 1. The dictionary containing the training patterns along with the trivial bases changes Eq. 1 as

$$y = \mathcal{T}\alpha + I\beta \tag{3}$$

where I represents the trivial bases and β represents the corresponding coefficients.

3.3. Sparse coefficients - Processing

For every test image, all possible sub-images of a priori fixed size are processed. For each sub-image, the Red channel image and the gray intensity images are independently processed. Each of them is expressed as a sparse linear combination of dictionary patterns, in l_1-framework. Hence for every sub-image, two sets of sparse coefficients are obtained, one for the red channel and the other for the gray

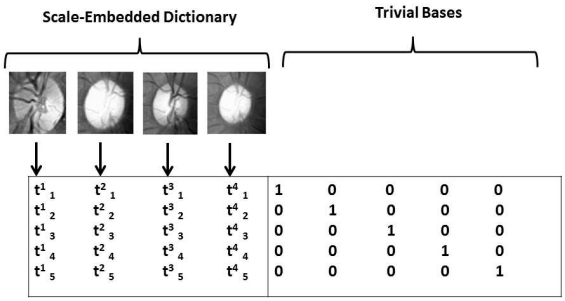

Fig. 1. Dictionary generation

intensity image. Let $\alpha_1, \alpha_2 \ldots \alpha_N$ denote the coefficient values corresponding to N basis elements containing OD at the center. Similarly let $\beta_{N+1}, \beta_{N+2} \ldots \beta_q$ denote coefficient values corresponding to the trivial basis elements. Here N is number of OD sub-images in the dictionary and q is the total number of dictionary entries including the trivial basis elements.

$$\begin{aligned} y^R &= \mathcal{T}\alpha^R + I\beta^R \\ y^Y &= \mathcal{T}\alpha^Y + I\beta^Y \end{aligned} \tag{4}$$

Here y_R and y_Y denote the array of sparse coefficients for Red channel and gray intensity images, respectively. For each of the sub-images, the information from an array of sparse coefficients is converted to a single value, called confidence measure, as given in Eq.(5). This value measures the likelihood of a given sub-image containing the OD at its center; higher the value, greater the likelihood. Hence for both the sparse coefficient sets, the respective confidence measures (η^R, η^Y) are obtained using Eq.(5).

$$\begin{aligned} \eta^R &= \frac{\sum_{i=1}^{N} \alpha_i^R}{\sum_{j=N+1}^{q} |\beta_j^R|} \\ \eta^Y &= \frac{\sum_{i=1}^{N} \alpha_i^Y}{\sum_{j=N+1}^{q} |\beta_j^Y|} \end{aligned} \tag{5}$$

To utilize information from both the sets of confidence measures, their dot product is obtained, $\eta = \eta^R.\eta^Y$. This will boost the high values further and suppress the smaller values, yielding a value of significance, where higher magnitudes indicate higher probability of presence of OD. The confidence values of each sub-image is rearranged over the 2D image grid in order to form the likelihood map indicating the probability of finding OD at each location. This map is convolved with Laplacian of Gaussian (LoG) blob detector and the location that results in peak response is declared as the location of the OD.

4. RESULTS

All programs were written in MATLAB. These programs were interfaced with the implementation of the sparse-coding routines, based on [10, 11], available at the website [12]. Multiple publicly available datasets like DIARETDB0 [13], DIARETDB1[14], and DRIVE [15] were used to test the proposed method. A representative example of the images used is shown in Fig. 2. The sequence of processing is outlined along with intermediate results on this example image. The image is down-sampled proportional to the down-sampling factor

Algorithm 1 Proposed OD Localization

1: Initialization: Create a dictionary A with atoms $\{t^1, t^2 \dots t^n\}$ from the training sub images (size : $n_1 \times n_2$). l_2-Normalize all columns of A.
2: For each sub image (size : $n_1 \times n_2$) of test image
3: **repeat**
4: Extract Red, Gray intensity images and vectorize to form y^R and y^Y.
5: Obtain the sparse coefficients for y^R and y^Y by solving the l_1-minimization problem as given in (2).
6: Compute confidence measures (η^R and η^Y) as given in 5.
7: Compute the combined confidence (η) measure using dot-product of η^R and η^Y.
8: **until** All sub-images are exhausted
9: Compute the combined confidence (η) measure using dot-product of η^R and η^Y.
10: Create the confidence map using η by overlaying on the image grid.
11: Use a blob detector over the confidence-map to localize the OD.

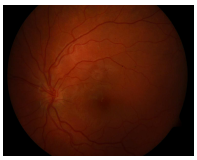

Fig. 2. An example image from the DIARETDB1 database

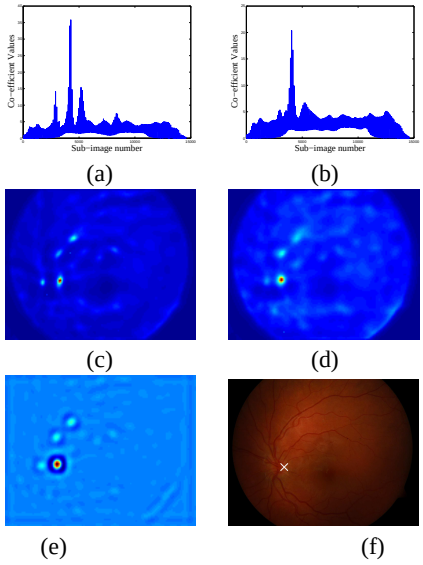

Fig. 3. Sequence of processing on an illustrative image (Fig. 2) from the DIARETDB1 database. Figs. (a)-(b) show plots of confidence measures for Red channel and gray intensity images, respectively. Figs. (c)-(d) show the re-shaped plots of confidence measures, respectively, to illustrate that their actual position is about the OD. Fig (e) shows the result of blob-detection on the dot-product of the two confidence measures. Fig. (f) shows the localized OD marked 'x'

used for dictionary creation. Red channel and gray intensity images are processed independently. The plots of the corresponding confidence measures are obtained using Eq.(5), shown in Figs.3(a) and 3(b), respectively. Re-shaping them as images for easy visualization we observe that the high values are seen about the actual position of the OD, in Figs.3(c-d). The dot product of the two confidence measures is obtained, on which a blob-detector Laplacian of Gaussian (LoG) is used to locate the OD, as shown in Fig.3(e). The localized OD is shown overlaid on the original image in Fig.3(f). Table 1 summarizes the performance of the method on each of the mentioned databases, along with the average computation time in seconds.

Table 1. Performance of the proposed method

Database	DB0	DB1	DRIVE	Overall
No. of images	130	89	40	259
Success	126	89	38	253
Accuracy (%)	96.9	100	95	97.6
Avg. Time (secs)	3.6	3.6	4.1	3.8

5. DISCUSSION

The databases chosen to illustrate the performance of the method show enormous variation across images. DIARETDB0 contains 130 images, of size 1200 $\times$ 901, of which only 20 are normal. The remaining 110 images contain signs of the diabetic retinopathy such as exudates and hemorrhages, leading to drastically varying levels of color and contrast. DIARETDB1 consists of 89 images, of size 1152 $\times$ 1500, of which 84 contain micro-aneurysms, while 5 are normal. DRIVE database consists of 40 images, of which 33 do not show any sign of diabetic retinopathy and 7 show signs of mild early diabetic retinopathy. These images are of size 584 $\times$ 565. As illustrated, the proposed method works satisfactorily well on all the three databases, with no need for any heuristic parameter tweaking during processing. The only constant that needs to be fixed at the start of a trial for a given database, is the scaling factor, in order to down-sample the image to an appropriate size in tune with those in the dictionary.

Figures 4 and 5 show results on the DRIVE database that have been illustrated in [16]. The results obtained using the two methods is comparable. However, the authors of [16] utilize 5 of the DRIVE images among the training images. In contrast, the proposed method outlined in this paper uses disjoint training and test data-sets. Figure 6 shows results on the DIARETDB0 and DIARETDB1 that have been illustrated in [17]. The results obtained using the two methods is comparable. As per the results tabulated by the authors, the accuracy obtained on DIARETDB0 is the same as that obtained by the proposed approach. However, on DIARETDB1, we obtain 100% accuracy, as against the authors reported method that failed on 2 of the images. Figs. 7(a) and 7(b) show examples from databases DIARETDB0 and DRIVE respectively, on which the proposed method failed. Clearly, in these images, the other blob-like structures distract the OD localizer. Dictionary creation holds the key to improved performance; hence care should be taken while creating the dictionary considering various challenges.

6. CONCLUSION

In this paper, a novel method for OD localization in fundal images is presented. The method is dictionary-based and poses the problem as one of classification, utilizing the discriminative property of sparse

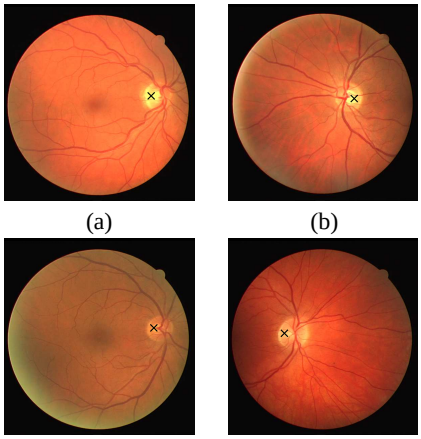

Fig. 4. Results of the proposed method on DRIVE. The 'x' indicates the OD center as detected by the proposed method.

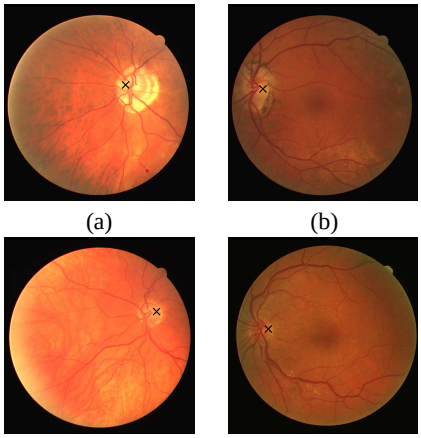

Fig. 5. Results of the proposed method on DRIVE. The 'x' indicates the OD center as detected by the proposed method.

representation. A scale-embedded dictionary is created with hand-marked sub-images containing OD at the center. For a given test-image, all sub-images of a priori size are expressed as linear combinations of dictionary patterns, minimizing the l_1-norm. These coefficients are processed to locate that sub-image which contains OD at its center. For every sub-image, the method processes Red-channel and gray intensity images, in parallel, utilizing their respective OD cues, fusing them eventually to yield robust OD localization. The performance of the proposed method is illustrated on publicly available databases such as DIARETDB0, DIARETDB1 and DRIVE.

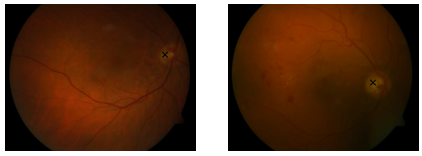

Fig. 6. Results of the proposed method on DIARETDB0. The 'x' indicates the OD center as detected by the proposed method.

Fig. 7. Example images on which the proposed method failed. The '+' indicates the OD center as detected by the proposed method.

7. REFERENCES

[1] T. Walter and J.C. Klein, "Segmentation of color fundus images of the human retina: Detection of the optic disc and the vascular tree using morphological techniques," in *Proceedings of the 2nd International Symposium on Medical Data Analysis*, 2001, pp. 282–287.

[2] Huiqi Li and Opas Chutatape, "Automatic location of optic disk in retinal images," in *Proceedings of the xxth International Conference on Image Processing*, 2001, pp. 837–840.

[3] W. Al-Nuaimy S. Sekhar and A. K. Nandi, "Automated localization of optik disk and fovea in retinal fundus images," in *Proceedings of the 16th European Signal Processing Conference (EUSIPCO)*, 2008.

[4] Aliaa Abdel-Haleim Abdel-Razik Youssif, Atef Zaki Ghalwash, and Amr Ahmed Sabry Abdel-Rahman Ghoneim, "Optic disc detection from normalized digital fundus images by means of a vessels direction matched filter," *IEEE Transactions on Medical Imaging*, vol. 27, no. 1, pp. 11–18, "Jan" 2008.

[5] Bob Zhang and Fakhri Karray, "Optic disc detection by multi-scale gaussian filtering with scale production and a vessels directional matched filter," *Medical Biometrics Lecture Notes in Computer Science*, vol. 6165, pp. 173–180, 2010.

[6] Mario Beaulieu Marc Lalonde and Langis Gagnon, "Fast and robust optic disc detection using pyramidal decomposition and hausdorff-based template matching," *IEEE Transactions on Medical Imaging*, vol. 20, no. 11, pp. 1193–1200, "Nov" 2001.

[7] J. Novo, M. G. Penedo, and J. Santos, "Optic disc segmentation by means of ga-optimized topological active nets," *Image Analysis and Recognition Lecture Notes in Computer Science*, vol. 5112, pp. 807–816, 2008.

[8] D. L. Donoho, "For most large underdetermined systems of linear equations the minimal l1-norm solution is also the sparsest solution," *Communications in Pure and Applied Math*, vol. 59, pp. 797–829, 2004.

[9] S. Chen, D. Donoho, and M. Saunders, "Atomic decomposition by basis pursuit," *SIAM Review*, vol. 43, no. 1, pp. 129–159, 2001.

[10] J. Mairal, F. Bach, J. Ponce, and G. Sapiro, "Online learning for matrix factorization and sparse coding," *Journal of Machine Learning Research,*, vol. 11, pp. 19–60, 2010.

[11] J. Mairal, F. Bach, J. Ponce, and G. Sapiro, "Online dictionary learning for sparse coding.," in *International Conference on Machine Learning*, 2009.

[12] WebLink, ," SPAMS, http://www.di.ens.fr/willow/SPAMS/downloads.html.

[13] WebLink, ," DIARETDB0, http://www2.it.lut.fi/project/imageret/diaretdb0/.

[14] WebLink, ," DIARETDB1, http://www2.it.lut.fi/project/imageret/diaretdb1/.

[15] WebLink, ," DRIVE, http://www.isi.uu.nl/Research/Databases/DRIVE/.

[16] Mira Park, Jesse S. Jin, and Suhuai Luo, "Locating the optic disc in retinal images," in *Proceedings of the International Conference on Computer Graphics, Imaging and Visualisation (CGIV'06)*, 2006, pp. 141–145.

[17] M. Usman Akram and Anam Tariq, "Automated optic disk localization and detection in colored retinal images," in *Proceedings of the 7th International Conference on Frontiers of Information Technology*, 2009.